Basin-Scale Consequences of Agricultural Land Use on Benthic Light Availability and Primary Production Along a Sixth-Order Temperate River

J. P. Julian,[1,2]* E. H. Stanley,[3] and M. W. Doyle[1]

[1]Department of Geography, University of North Carolina, Chapel Hill, North Carolina, USA; [2]Department of Geography, University of Oklahoma, Norman, Oklahoma, USA; [3]Center for Limnology, University of Wisconsin, Madison, Wisconsin, USA

ABSTRACT

The emerging spatial scale of interest for fluvial ecosystem studies and applications is the river basin. Although much focus has been directed toward habitat availability and nutrient cycling across the fluvial landscape, light availability has received considerably less attention and has not been assessed quantitatively at the basin-scale despite it being the primary energy source for aquatic ecosystems. We developed a basin-scale light availability model that couples readily available broad spatial data with easily measured synoptic data using a GIS framework and the principles of hydraulic geometry. We used this model to (i) quantify benthic light availability (E_{bed}) along a 160-km river in central Wisconsin, USA, (ii) predict gross primary production (GPP) along the same river, and (iii) assess the effects of agricultural land use on E_{bed} and GPP. Overall, E_{bed} decreased in the downstream direction due primarily to increased turbidity, and there was considerable local variation caused by changes in topography, riparian vegetation, and channel orientation. These local variations in E_{bed} caused GPP to fluctuate greatly over short distances, as much as 2.1 g C m^{-2} d^{-1} over 260 m. When summed over the entire channel length, present-day, post-agricultural GPP (635 kg C d^{-1}) was about eight times lower than estimated pre-agricultural GPP (4992 kg C d^{-1}). Model simulations revealed that agricultural land use can cause an order of magnitude change in GPP, reduce or increase inter-sectional variability in GPP, and significantly alter broad spatial trends in GPP. Our basin-scale benthic light availability model is a tool that researchers can use to investigate relationships between light availability and ecosystem processes at broad spatial scales and also one that practitioners can use for more holistic fluvial ecosystem assessments.

Key words: GPP model; solar radiation; hydrogeomorphic controls; riparian vegetation shading; channel geometry; turbidity.

INTRODUCTION

Large-scale changes in land use have a range of consequences for aquatic ecosystems, the most conspicuous of which may be nutrient enrichment

and enhancement of primary production (that is, eutrophication). Although all types of aquatic ecosystems have been subject to nutrient enrichment, studies of eutrophication are dominated by lakes and coastal zones, and parallel work on rivers and streams is conspicuously scarce (Alexander and Smith 2006; Hilton and others 2006). Attempts to quantify relationships between nutrient status and algal growth, or to use these two variables to assess trophic status have been less successful for lotic than for lentic ecosystems (Lin and others 2007). In part, this limited success likely results from the reality that primary production in streams and rivers is often limited by controls other than nutrients, chief among which is light (Dodds and Welch 2000; Hilton and others 2006).

Spatial and temporal trends in benthic light availability have been altered by various anthropogenic disturbances (Davies-Colley and others 2003), but most intensively by agricultural practices. Accelerated soil erosion due to agriculture has been the main contributor of increased turbidity to most rivers around the world (Walling and Fang 2003), and has decreased benthic light availability by enhancing water column light attenuation. Conversely, agricultural land conversion has also caused the widespread removal of riparian forests (MEA 2005), which increases benthic light availability through reduced shading. These alterations are likely to be discontinuous in space and time, further complicating trends in benthic light availability.

Despite the fundamental role of light availability in controlling metabolism in lotic ecosystems, there has been limited progress in understanding when, where, and how light availability affects primary production, and how the relationship between light and metabolism is altered by the suite of conditions associated with agricultural land use in the surrounding basin (Roberts and others 2007; Von Schiller and others 2007). This critical gap exists because (i) light has not been widely recognized as a limiting resource in riverine ecosystems in comparison to nutrients and habitat, (ii) the optical water quality of rivers is highly variable and difficult to characterize, and (iii) boundary conditions (banks, riparian vegetation) make ambient light measurements difficult (Davies-Colley and others 2003).

Because land-use changes generally occur at relatively large spatial scales, developing a robust understanding of how light availability may affect metabolism in rivers also needs to proceed at this same scale. Although landscape-scale frameworks of both physical and ecological patterns have a long history in studies of fluvial systems (for example, Leopold and Maddock 1953; Vannote and others 1980), a quantitative landscape model of riverine light regimes does not exist. Qualitative predictions have been made regarding general longitudinal patterns of light in rivers (Vannote and others 1980), but explicit tests of these predictions are scarce. Thus, we have limited information available to answer basic questions such as: What are characteristic patterns and variance in light availability along streams and rivers? How do physical attributes such as channel form or orientation affect light availability? Is light availability more strongly affected by terrestrial shading or optical characteristics of water? To begin addressing these questions, we demonstrate how basin-scale riverine light availability can be characterized by combining the reach-scale benthic light availability model (BLAM; Julian and others 2008b) with principles of hydraulic geometry (sensu Leopold and Maddock 1953) within a GIS framework. Next, we coupled this GIS-based model with light-metabolism equations to quantify gross primary production (GPP) along the length of a sixth-order temperate river in an agriculturally dominated basin. Finally, we use this coupled model to ask: how do different components of agricultural land use in the form of altered riparian structure and elevated turbidity affect a river's light regime and metabolism?

METHODS

Study Area

The Baraboo River provides an ideal case study to investigate light along the natural river continuum because its entire 187-km mainstem is free-flowing with no impoundments. It historically had nine dams on its mainstem, but all have been removed, the last one in 2001 (WDNR 2006). The Baraboo River is a sixth-order stream that begins in the Western Uplands of Wisconsin (WI, USA) and meanders through the non-glaciated Driftless Area of central WI before it empties into the Wisconsin River near Portage, WI (Figure 1). It drops in elevation from 420 to 235 m above mean sea level over its length of 187 km. Its 1690-km^2 drainage basin is mostly agriculture (47%), followed by forest (31%), grassland (15%), wetland (5%), urban (1%), and barren (1%) (WDNR 1998). The pre-settlement landcover was dominated by southern oak forest (*Quercus alba*, *Q. velutina*, and *Q. rubra*) in the uplands and oak savanna (characterized by *Q. macrocarpa*, *Q. alba*, *Q. bicolor*, and *Andropogon gerardii* and mixed forbs in the ground layer) in the lowlands
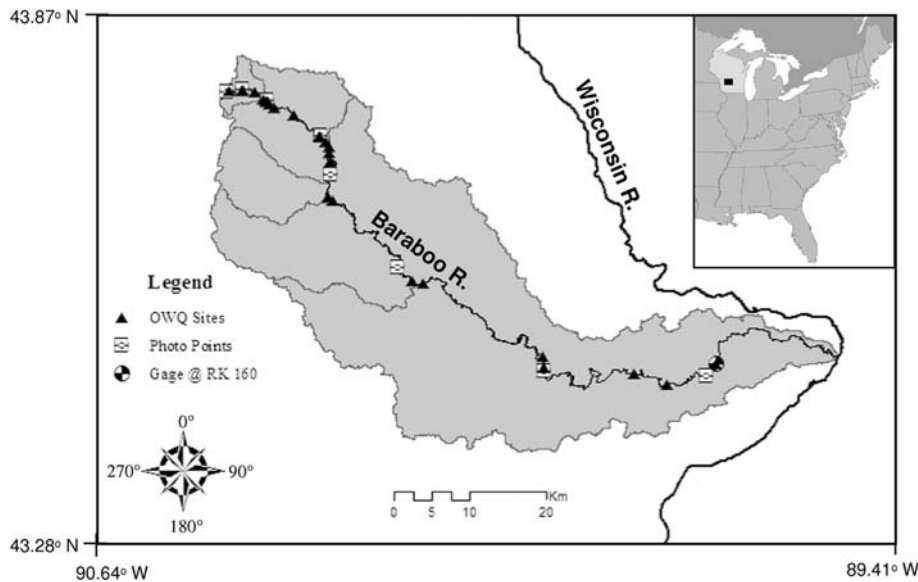
Figure 1. Baraboo River Basin, Wisconsin, USA. Major tributaries are depicted. Gage represents the downstream extent of this study. Photo points are locations where canopy photos were taken and channel width and depth measured. Optical water quality (OWQ) sites are locations where turbidity was measured. Compass in *bottom-left* corner provides context for channel orientation.

(Curtis 1959). The riparian corridor of Baraboo River is currently composed mostly of mixed-hardwood forest and various grasses. The hydrology of the basin is dominated by thunderstorm frontal systems, resulting in a relatively flashy hydrologic regime, although seasonal flooding is common in spring due to snowmelt events. The flow gage (USGS #05405000) at RK 160 (160 river kilometers downstream of the headwaters) represents the downstream extent of our analysis (Figure 1).

Modeling Basin-Scale Benthic PAR

BLAM (Julian and others 2008b) calculates the amount of photosynthetically active radiation (PAR) at the riverbed (E_{bed}) by incorporating the terrestrial and aquatic controls on benthic light availability:

$$E_{bed} = (E_{can} \cdot s \cdot r)e^{-K_d \cdot y} \tag{1}$$

where E_{can} is above-canopy PAR in mol m^{-2} day^{-1}, s is the shading coefficient, r is the reflection coefficient, K_d is the diffuse attenuation coefficient for underwater PAR in m^{-1}, and y is water depth in m. This empirical model was designed for the reach scale, where K_d is assumed to remain constant and s collectively includes shading from topography and riparian vegetation. To apply this approach to the basin scale, we (i) allowed K_d to vary along the river; (ii) divided s into the topographic shading coefficient (s_t) and the vegetation shading coefficient (s_v), where $s = s_t \cdot s_v$; and (iii) used a GIS-based analysis to extrapolate BLAM to the entire 160-km mainstem river channel.

The conceptual framework of our GIS-based approach for quantifying E_{bed} is presented in

Figure 2. We overlaid a hydrography dataset of the Baraboo River onto a digital elevation model (DEM) and land-cover map (LCM) to calculate s_t and s_v, respectively. We then conducted a synoptic survey of the Baraboo River, measuring channel width and depth, turbidity, and canopy structure. We incorporated these empirical data into our GIS framework and used equation (1) to derive E_{bed}.

Model Parameters

Above-Canopy PAR (E_{can})

Above-canopy PAR is the amount of light available to the river before any terrestrial shading. We modeled E_{can} with *Gap Light Analyzer* (GLA; Frazer and others 1999), using the parameters in Table 1 and the center of the drainage basin as our location and elevation. We kept E_{can} spatially constant across the basin so that variations in the other parameters could be assessed independently. From GLA, we derived an average daily E_{can}, in mol m^{-2} day^{-1}, for the Baraboo River Basin during May 15–Sep 15, which corresponds to the period of more than 90% maximum leaf area index (that is, at least 90% of the leaves were on the trees). To assess the average and range of E_{bed}, we also obtained actual daily E_{can} values from a USDA weather station located in Dancy, WI (WI02; USDA 2007), which reported 3-min averages of 20-s readings from a *LI-COR* quantum sensor.

Topographic Shading Coefficient (s_t)

Topography is the first terrestrial control that reduces the amount of light available to the river. We calculated daily average s_t (the proportion of PAR
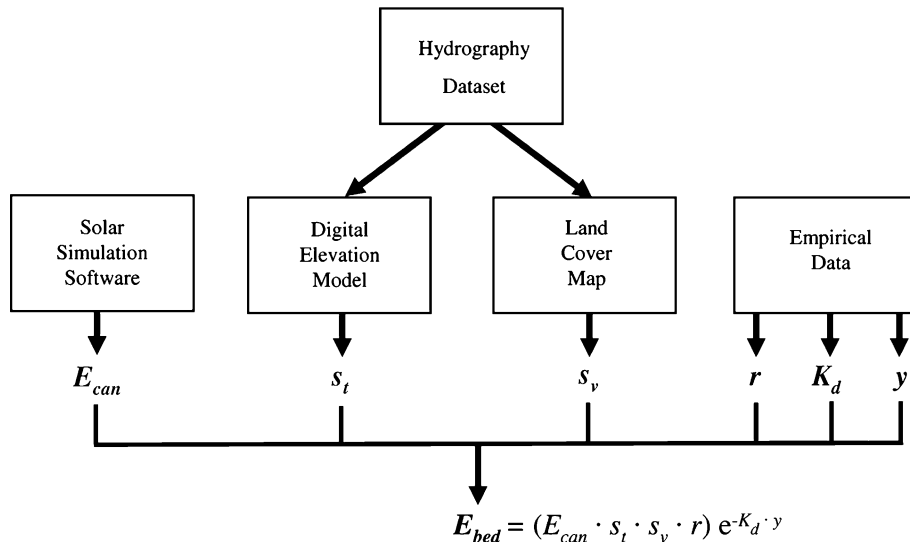
$$E_{bed} = (E_{can} \cdot s_t \cdot s_v \cdot r) \, e^{-K_d \cdot y}$$

available to the river after topographic shading) using *Solar Analyst 1.0* (Fu and Rich 2000; Table 1), which uses a view-shed algorithm to compute the proportion of E_{can} that reaches the surface of every cell in a DEM after shading effects from elevation, shadows, and atmospheric conditions. We used a USGS DEM (cell-size: 30 × 30 m) in combination with a raster of the Baraboo River mainstem (cell-size: 30 × 30 m) to extract s_t for each 30-m segment of the river. We created this river raster by converting the national hydrography dataset of the Baraboo River (scale: 1:24,000) into a raster using *Arc Hydro* (Maidment 2002). *Arc Hydro* also assigned every cell in the river raster an azimuthal channel orientation (flow direction) based on the eight compass directions. For example, a river cell flow-

ing into a cell directly below it (N–S) had an orientation of 180°. Because each river cell had some sinuosity, we normalized raster river distance to actual distance by assigning horizontal/vertical cells (0, 90, 180, and 270°) 33.6 m and diagonal cells (45, 135, 225, and 315°) 47.5 m. These distances were calculated using the Pythagorean theorem and assuming the total distance adds up to 160 km. From this mainstem river raster, we calculated a longitudinal profile of s_t along the Baraboo River.

Vegetation Shading Coefficient (s_v)

After topographic shading, the next control that reduces the amount of light available to the river is riparian vegetation. We calculated daily average s_v (the proportion of PAR available to the river after vegetation shading) using a LCM of the Baraboo River Basin (WDNR 1998) in combination with canopy photos analyzed with GLA (Frazer and others 1999; Table 1), which computes the proportion of E_{can} that reaches the water surface after shading by the canopy. Digital hemispherical canopy photos were collected using a *Nikon Coolpix 4500* with fisheye lens. We took canopy photos at eight transects along Baraboo River (Figure 1) on Aug 18, 2006. Transects were selected based on changes in channel width and canopy structure. The canopy photos were corrected for topographic shading by dividing the *s* value from *GLA* by s_t ($s_v = s/s_t$), which we obtained from the longitudinal profile of s_t. By performing this correction, we prevented topographic shading from being incorporated into our model twice.

We used the canopy photos to construct empirical relationships between s_v and channel width for

Table 1. *Gap Light Analyzer* (GLA) and *Solar Analyst* (SA) User-defined Parameters

Parameter	GLA	SA
Period	May 15–Sep 15	May 15–Sep 15
Projection	Polar	Polar
Orientation	Horizontal	Horizontal
Time step	1 min	30 min
Azimuth regions	36	8
Zenith regions	9	8
Solar constant	1367 W/m^2	1367 W/m^2
Cloudiness index	0.50	na
Spectral fraction	0.45	na
Beam fraction	0.50	0.50
Sky-region brightness	UOC model	UOC model
Clear-sky transmission coefficient	0.60	0.60

Options not available in the software are labeled "na."

the eight different channel orientations (0, 45, 90, 135, 180, 225, 270, and 315°). Active channel width (sensu Osterkamp and Hedman 1977) measured at each photo location was used to construct a width rating curve based on distance from the headwaters so that we could assign every cell in the river raster a width based on this rating curve. We calculated the variation in s_v with channel orientation by rotating the canopy photos in 45° increments and then reanalyzing in GLA (sensu Julian and others 2008b), which we then used to construct a separate rating curve for each channel orientation. These curves were derived from least squares power regression of four canopy photos. Half-canopy s_v curves were derived from transects where one bank was forested and the other deforested. To normalize the half-canopy photos, we rotated each photo so that the forested bank was on the right bank looking downstream (that is, for a channel orientation of 90°, the south bank was forested). Full-canopy s_v curves were derived from transects where both banks were forested. Due to limited full-canopy photos from the Baraboo River for intermediate widths, two of the full-canopy photos were obtained from Deep River, NC, which was also a sixth-order river with a similar riparian corridor (mixed-hardwood forest) and channel width (~40 m; Julian and others 2008b). This substitution assumes that canopy shading attributes were comparable between sites.

Using the LCM, each cell in the Baraboo River raster was classified as having a full-canopy, half-canopy, or no canopy. Canopy classifications were assigned on the basis of whether or not a forest land-cover cell was adjacent to the river cell. For example, a river cell with a forest land-cover cell adjacent to its right bank and a non-forest land-cover cell adjacent to its left bank was classified as having a half-canopy. Using the river raster's attributes of width, channel orientation, and canopy cover, we calculated s_v for each river cell based on the rating curves described above. For cells with no canopy (that is, neither adjacent cell was a forest land cover), we used an s_v of 1.0.

Reflection Coefficient (r)

After terrestrial shading by topography and riparian vegetation, the amount of available light is further reduced by reflection at the air–water interface. We used a daily average r (the proportion of PAR that enters the river after reflection) of 0.88, which we obtained from a previous study in a nearby basin (Julian and others 2008b). The range of r in this previous study was 0.84–0.96.

Diffuse Attenuation Coefficient (K_d)

Once light enters the water column, it is attenuated exponentially with depth at a rate defined by K_d. We estimated K_d along the Baraboo River from nephelometric turbidity (T_n) measurements, where $K_d = 0.17 T_n$ (Julian and others 2008b). We measured T_n with a *HACH* 2100P turbidimeter from water samples collected at 22 locations along the Baraboo River on Aug 13, 2006 during baseflow (Figure 1). From these measurements, we constructed a K_d rating curve based on distance from the headwaters.

Water Depth (y)

The amount of light that reaches the riverbed is ultimately dictated by the depth of the river. We quantified y at each photo location, using the average of three depth measurements taken in the center of the channel and approximately three channel widths apart. From these measurements, we constructed a y rating curve based on distance from the headwaters (sensu Leopold and Maddock 1953). All empirical data collected along the Baraboo River were georeferenced in GIS using a *Garmin* GPS.

Model Assumptions

We used equation (1) in conjunction with E_{can} from GLA, the longitudinal profile of s_t, the s_v curves, an r of 0.88, the K_d rating curve, and the y rating curve to calculate E_{bed} for every cell ($n = 3980$) in the Baraboo River raster. These values of E_{bed} are summer daily averages, in mol m^{-2} day^{-1}, based on the average daily E_{can} for May 15–September 15, 2006. The cell size of the river raster set the spatial resolution of E_{bed} at approximately 30 m. Our calculation of E_{bed} assumed that width, depth, and turbidity increased consistently in the downstream direction. Therefore, local variations in width, y, and K_d were not taken into account. Determination of s_v assumed the LCM accurately delineated riparian forests, and canopy structure (height, density) was constant for all forested riparian cells. Finally, because empirical data were collected from the center of the channel during baseflow, E_{bed} is only representative of the channel centerline during baseflow.

Primary Productivity

Gross primary productivity can be predicted with PAR measurements and community-specific photosynthesis–irradiance (P–I) relationships (Jassby and Platt 1976). We simulated GPP for cyanobac-

teria because this group often dominates periphyton in agricultural streams in Wisconsin (Scudder and Stewart 2001). Photoinhibition for benthic cyanobacteria was assumed to be negligible (Dodds and others 1999), and therefore the method of Jassby and Platt (1976) was used in combination with the P–I areal parameters for riverine cyanobacteria (Dodds and others 1999). GPP was calculated as carbon-specific production in g C m^{-2} d^{-1}, with a conversion factor of 0.375 O_2 for C. PAR measurements were obtained from a nearby weather station (WI02; USDA 2007) for the day of August 21, 2006, which was equivalent to the daily average PAR for the study period and had varying cloudiness. PAR measurements were also used from June 4 and September 11, 2006 to obtain GPP for days with full sun and complete overcast, respectively. We calculated GPP in 3-min intervals and then integrated to obtain daily values of GPP for each cell in the river raster ($n = 3980$). Raster values were summed and multiplied by river surface area to estimate whole-river production.

Model Simulations

We assessed the effect of agricultural land use on E_{bed} and GPP for Baraboo River through three model simulations. The first simulation was intended to reproduce pre-agricultural conditions by assuming the entire riparian zone was forested and water clarity was pristine. We obtained pristine K_d values from a longitudinal survey of water clarity along the Motueka River (Davies-Colley 1990), a relatively undeveloped basin in New Zealand where most of its area was conservation land (55%), followed by production forestry (25%) and low intensity sheep/cattle farming (19%) (Basher 2003). We converted water clarity measurements to K_d using the conversion factors in Davies-Colley and others (2003, p. 76). Our justification for using the Motueka River Basin is that it had a similar area (2180 km^2) and shape (pear-shaped) as the Baraboo River Basin, because basin morphometry is a major driver in water chemistry (Benda and others 2004; Julian and others 2008a). That is, we assumed that longitudinal trends in water clarity of the Motueka River were a reasonable representation of pristine (pre-agricultural) trends in the physically similar Baraboo River. Further, we used median water clarity values from the Motueka River to provide a conservative estimate of pristine baseflow conditions in Baraboo River. To simulate a longitudinally continuous riparian forest along Baraboo River, we created a modified LCM where every adjacent cell to the river raster was classified as forest.

The second simulation included effects of increased soil runoff associated with farming by using present-day turbidity values but maintaining a continuous forested riparian buffer. We simulated the continuous riparian forest using the method above, but used the K_d values from our longitudinal survey of turbidity along the Baraboo River rather than pristine values. The objective of the third scenario was to simulate both high turbidity and riparian deforestation. To simulate a completely deforested riparian zone, we created a modified LCM where every adjacent cell to the river raster was classified as non-forest.

Temporal changes in topography and channel orientation were not simulated, and thus assumed constant among scenarios. Additionally, GPP calculations did not take into account temporal changes in nutrient availability, which would especially be different between pre- and post-agricultural scenarios. Comparisons among the three model simulations, along with the actual longitudinal profiles of present-day Baraboo River, therefore illustrate changes of E_{bed} and GPP in response only to changes in riparian vegetation and water clarity.

RESULTS

Empirical Parameters from Synoptic Survey

Channel Geometry

Active channel width along the Baraboo River continuum increased systematically at a rate of $0.23\ RK^{1.00}$, with a maximum of 40 m at RK 160 (Figure 3A). Baseflow channel depth along the river also increased systematically at a rate of $0.06RK^{0.65}$, with a maximum of 1.5 m at RK 160 (Figure 3B). Vertical channel incision was minimal in the upper reaches of Baraboo River, but increased steadily in the downstream direction, attaining a maximum of 4 m at RK 160.

Water Clarity

The headwaters of Baraboo River were optically clear with a minimum T_n of 1.44 NTU, which converted to a K_d of 0.24 m^{-1} (Figure 4A). Between RK 6 and RK 74, K_d increased rapidly in the downstream direction. The lower reaches of Baraboo River were very turbid with a maximum K_d of 6.16 m^{-1}. After RK 74, K_d leveled off and then decreased slightly over the last 18 km of the study area. The spatial trend in K_d was largely dictated by the locations of major tributary junctions (see Figure 1), as tribu-
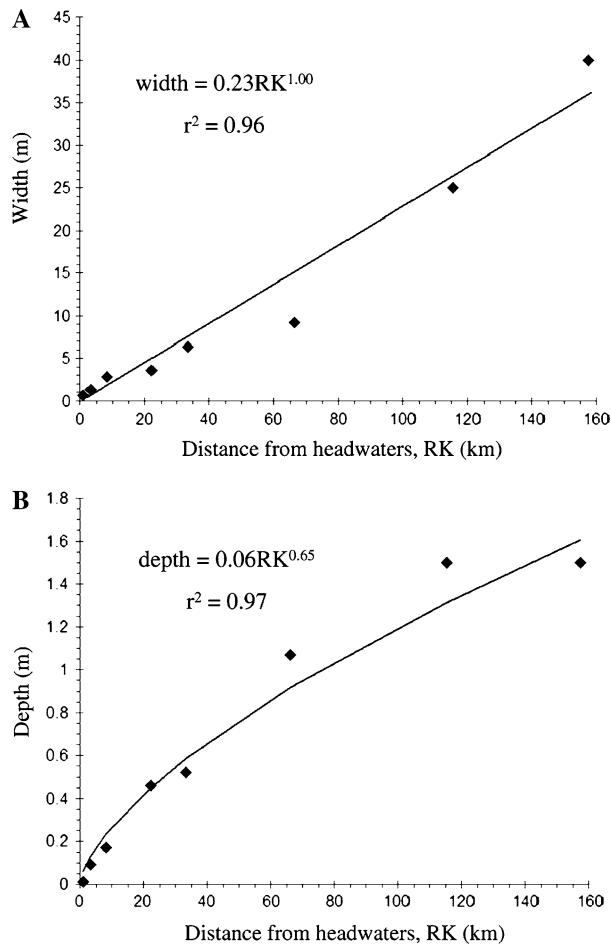
A

width = $0.23RK^{1.00}$

$r^2 = 0.96$

B

depth = $0.06RK^{0.65}$

$r^2 = 0.97$

Figure 3. Downstream variation in active channel width (**A**) and depth (**B**) along Baraboo River on August 18, 2006.

taries were sources of suspended particulates (Julian and others [2008a]). The trend in K_d along the Baraboo River continuum was best characterized by a third-order polynomial ($r^2 = 0.93$, Figure [4]A), which has been shown to be typical of pear-shaped basins (Julian and others [2008a]).

Modeled Parameters from GIS Analysis

Incoming PAR

Between May 15 and September 15, 2006, daily above-canopy PAR (E_{can}) in central Wisconsin (WI02; USDA [2007]) fluctuated considerably in response to varying degrees of cloudiness, ranging from 5.04 (complete overcast) to 59.91 mol m^{-2} d^{-1} (full sun). Average E_{can} was 41.98 ± 13.88 mol m^{-2} d^{-1} (mean ± sd). GLA-modeled E_{can} for this same period was 39.85 mol m^{-2} d^{-1}, only a 5% difference from the measured average.
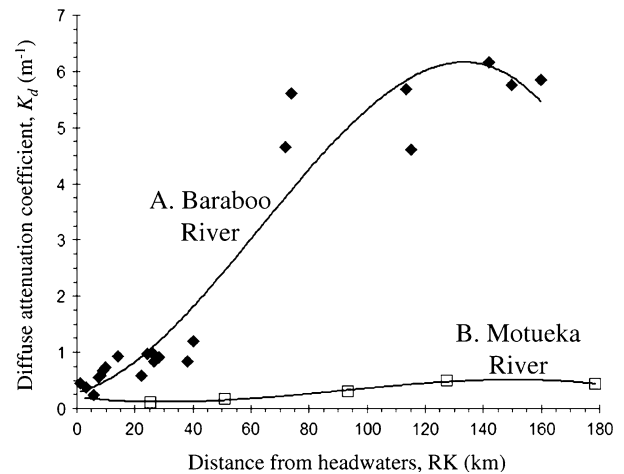

Figure 4. Downstream variation in the diffuse attenuation coefficient (K_d) for Baraboo River, WI, USA on August 13, 2006 (**A**) and Motueka River, NZ (**B**). Baraboo River is in an agriculturally dominated basin, whereas Motueka R. is in a relatively undisturbed basin. Distance for Motueka River was normalized to that of Baraboo River. Data for Motueka River adapted from Davies-Colley ([1990]). Baraboo River: $K_d = -4.21E-06RK^3 + 7.93E-04RK^2 + 0.01RK + 0.29$, $r^2 = 0.93$; Motueka River: $K_d = -3.57E-07RK^3 + 9.09E-05RK^2 - 3.11E-03RK + 0.12$, $r^2 = 0.99$.

Topographic Shading

The topographic shading coefficient (s_t) fluctuated around a mean of 0.94 ± 0.01 (Figure [5]). Most of this 6% shaded PAR occurred near dusk when the Western Uplands blocked incoming PAR from the western horizon (compare Figures [1] and [5] for context). The low values of s_t were associated with high cliffs or hills. For example, the section of river with the greatest topographic shading (RK 32, $s_t = 0.75$) was located on the north side of Kimballs Bluff, a hill that was 30 m higher than the river's elevation. The extended section with high topographic shading (RK 112-119) traversed through the Upper Narrows of the North Range Baraboo Hills, where high cliffs bordered the river. The high values of s_t, which were mostly located near the headwaters and lower reaches, occurred in areas where topographic shading was minimal. Overall, topographic shading along the river was small, with only locally significant effects.

Riparian Vegetation Shading

Riparian vegetation along Baraboo River was highly variable and discontinuous. Along the 160-km study area, 90.5 km had no canopy (neither bank forested), 31.0 km had a half-canopy (one bank forested, one bank deforested), and 38.5 km
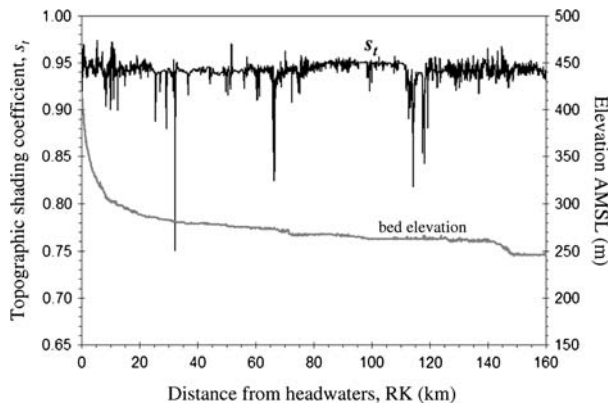
Figure 5. Topographic shading and bed elevation along the Baraboo River. Both variables were extracted from a USGS 30-m DEM. The average s_t of 0.94 was largely due to shading by the Western Uplands, which blocked incoming PAR from the western horizon.

had a full-canopy (both banks forested). In full-canopy sections, the vegetation shading coefficient (s_v) ranged from 0.16 to 0.77, and increased systematically with channel width (that is, riparian shading decreased with increasing channel width). In half-canopy sections, s_v (range 0.20–0.83) also increased systematically with channel width, but at a lower rate (Figure 6).

The planform of Baraboo River was extremely sinuous, resulting in frequent changes in channel orientation (Figure 1). Of the 3980 river raster cells, channel orientation changed 1958 times. A majority of the channel sections had either a 90° (29%) or 135° (25%) orientation, which is consistent with the NW–SE basin orientation. For full-canopy sections, the effect of channel orientation on s_v was minimal near the headwaters and increased with increasing channel width (Figure 6A). For example, there was no difference in s_v between 90° and 180° at a width of 1 m, but at a width of 40 m, s_v for 90° was 0.14 greater than for 180°. This divergent trend in s_v for full-canopy sections resulted from closed canopies at small channel widths mitigating the effect of channel orientation (Julian and others 2008b). Overall, E–W channels (90°) had the highest s_v, and N–S channels (180°) had the lowest s_v for full-canopy sections.

For half-canopy sections, the effect of channel orientation on s_v was considerable at all channel widths (Figure 6B). For example, there was a 0.20 difference in s_v between 270° and 90° at a width of 3 m, and there was a 0.19 difference in s_v between 270° and 90° at a width of 40 m. This approximate parallel trend in s_v for half-canopy sections resulted from the absence of a closed canopy at any channel
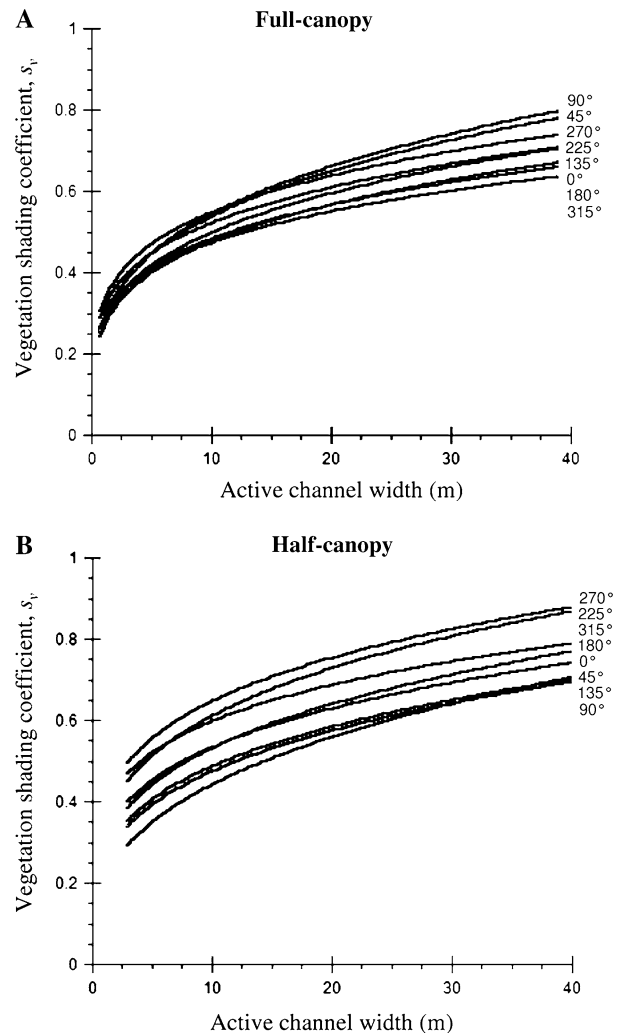

Figure 6. Vegetation shading coefficient (s_v) curves based on channel width and orientation. Full-canopy curves (**A**) are for transects with two forested banks. Half canopy curves (**B**) are for transects with one forested bank and one deforested bank. For transects with two deforested banks (no canopy), $s_v = 1.0$.

width. Overall, channels with northern forested banks (270°) had the highest s_v, and channels with southern forested banks (90°) had the lowest s_v for half-canopy sections.

Benthic PAR and GPP along Baraboo River

Benthic PAR (E_{bed}) along Baraboo River was highly variable, but generally decreased in the downstream direction (Figure 7A). Maximum E_{bed} (33.05 mol m^{-2} d^{-1} or 83% of incoming PAR) occurred at RK 0.5, which was deforested ($s_v = 1.00$) and optically clear ($K_d = 0.29$ m^{-1}). Benthic GPP also decreased in the downstream
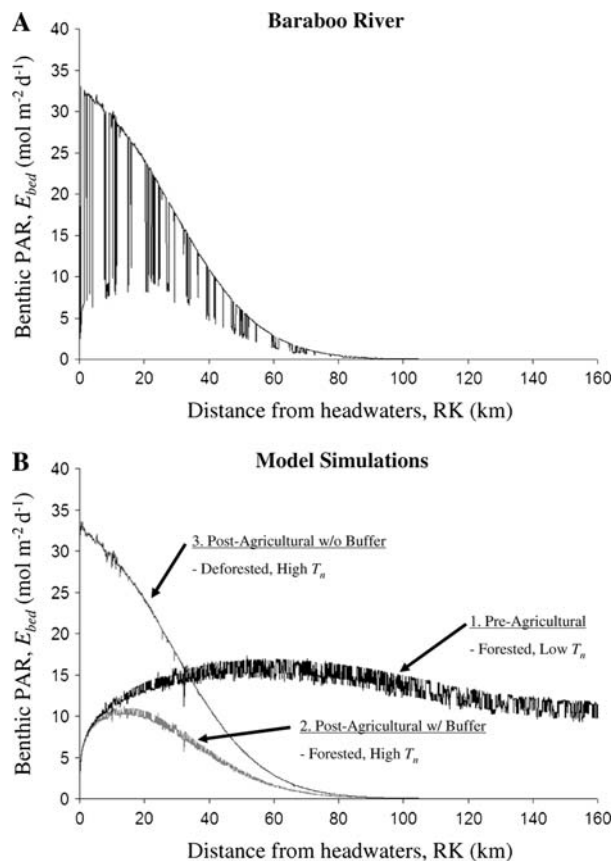
Figure 7. Benthic PAR along the Baraboo River (**A**) and under model simulations (**B**). The degree of riparian cover and turbidity (T_n) is labeled for each simulation. All four curves were calculated for the average summer day (E_{can} = 39.85 mol m^{-2} d^{-1}).
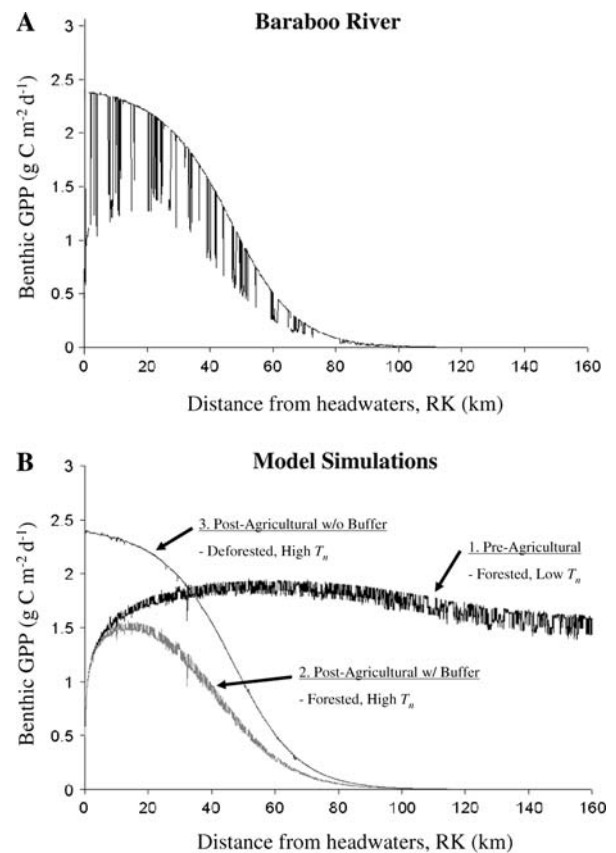

Figure 8. Benthic GPP along the Baraboo River (**A**) and under model simulations (**B**). GPP was calculated using the method of Jassby and Platt (1976), the photosynthesis–irradiance curve for cyanobacteria (Dodds and others 1999), and the E_{bed} distributions of Baraboo River.

direction with decreasing E_{bed} (Figure 8A); however, their rates of decline were not longitudinally equivalent. Over the first 30 km, spatially averaged GPP decreased by 3% whereas spatially averaged E_{bed} decreased by 32%. Over the next 30 km, the two variables decreased by similar amounts, 78% and 92% for GPP and E_{bed}, respectively. The different trend in GPP over the first 30 km resulted from the asymptotic trend of the P–I curve for riverine cyanobacteria (that is, above 20 mol m^{-2} d^{-1}, GPP did not increase significantly). GPP was effectively extinguished by RK 101, just 15 km upstream of E_{bed} extinction. At this point in the river, the high turbidity of the water column (K_d = 5.70 m^{-1}) negated any effects of the terrestrial controls (topography, riparian vegetation, or channel geometry) on benthic light availability.

Upstream of RK 116, riparian vegetation was responsible for most of the spatial variability in E_{bed} along Baraboo River. For example, two adjacent cells at RK 0.5 (one with no canopy, one with half-

canopy) with the same orientation (90°), width (0.11 m), y (0.04 m), s_t (0.95), and K_d (0.29 m^{-1}) displayed an order of magnitude difference in E_{bed} (33.05 vs. 3.27 mol m^{-2} d^{-1}, respectively). Consequently, fluctuations in benthic GPP were most extreme in the headwaters of Baraboo River, ranging from 0.3 to 2.4 g C m^{-2} d^{-1} over the first 0.5 km. As the canopy opening increased with distance downstream (via increased channel width), the variability in GPP decreased. Following riparian vegetation, channel orientation caused the next greatest variation in GPP along the continuum. For example, two nearby cells at RK 15 (one at 90°, one at 180°) with the same riparian vegetation (half-canopy right bank), width (3.48 m), y (0.35 m), s_t (0.94), and K_d (0.59 m^{-1}) displayed a 20% difference in GPP (1.28 vs. 1.53 g C m^{-2} d^{-1}, respectively). Topography caused considerable local differences in GPP. Kimballs Bluff at RK 32, for example, reduced GPP from 1.89 to 1.68 g C m^{-2} d^{-1} over a distance of 0.1 km (s_t was the only
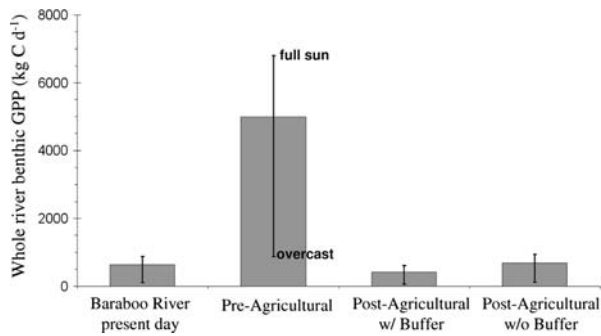
Figure 9. Whole river benthic GPP for Baraboo River and agricultural land-use scenarios for the average summer day during baseflow. Maximum error bars represent full sun conditions and minimum error bars represent complete overcast conditions.

parameter that varied over this distance). Because width, y, and K_d were modeled using rating curves, variability in GPP caused by local variations in these parameters was not assessed.

Whole river GPP for the 160-km Baraboo River was 635 kg C d^{-1} (Figure 9). This value was calculated using the PAR distribution from the average summer day, one with an intermediate level of cloudiness (E_{can} = 39.85 mol m^{-2} d^{-1}). The range of primary production for varying atmospheric conditions was considerable. Under full sun conditions (E_{can} = 59.91 mol m^{-2} d^{-1}), whole river GPP was 880 kg C d^{-1}. Under complete overcast conditions (E_{can} = 5.04 mol m^{-2} d^{-1}), whole river GPP was 114 kg C d^{-1}, almost an eightfold decrease from full sun conditions.

Benthic PAR and GPP Under Model Simulations

Pre-agricultural

The longitudinal distribution of E_{bed} along Baraboo River with a completely forested riparian corridor and pristine water clarity followed a parabolic trend where E_{bed} was low in the headwaters, high in the middle reaches, and declined slightly in the lower reaches (Figure 7B, curve 1). The value of GPP began with 0.50 g C m^{-2} d^{-1} at RK 0, attained a maximum of 1.96 g C m^{-2} d^{-1} at RK 52, and ended with 1.43 g C m^{-2} d^{-1} at RK 160 (Figure 8B, curve 1). Because riparian vegetation remained constant along the continuum, this trend of primary production was dictated by the trends of channel width (Figure 3A), depth (Figure 3B), and K_d (Figure 4B). Inter-sectional variability (vertical scatter around the mean) was caused mostly by channel orientation (Figure 6A) and occasionally

by topography (for example, RK 32). This variation in GPP with channel orientation increased with distance downstream, attaining a maximum difference of 0.21 g C m^{-2} d^{-1} between adjacent cells.

Post-agricultural with Riparian Buffer

The longitudinal distribution of E_{bed} along Baraboo River with a completely forested riparian corridor and higher turbidity followed a parabolic trend where E_{bed} was low in the headwaters, high in the middle reaches, and essentially zero in the lower reaches (Figure 7B, curve 2). The value of GPP began with 0.50 g C m^{-2} d^{-1} at RK 0, attained a maximum of 1.57 g C m^{-2} d^{-1} at RK 14, and reached a minimum of less than 0.01 g C m^{-2} d^{-1} at RK 97 where it remained for the last 63 km (Figure 8B, curve 2). Like the previous simulation where riparian vegetation remained constant along the continuum, this trend of primary production was dictated by the trends of channel width (Figure 3A), depth (Figure 3B), and K_d (Figure 4A). The higher K_d values in this simulation due to higher turbidity mitigated the effect of channel orientation on GPP (that is, less vertical scatter around the mean), with only a maximum difference of 0.12 g C m^{-2} d^{-1} between adjacent cells. Compared to the pre-agricultural simulation, GPP in this simulation had a lower peak that was shifted 38 km upstream.

Post-agricultural with No Riparian Buffer

The longitudinal distribution of E_{bed} along Baraboo River with a completely deforested riparian corridor (s_v = 1.00) and higher turbidity followed a logarithmic trend where E_{bed} was very high in the headwaters and decreased with distance downstream (Figure 7B, curve 3). The value of GPP began with 2.40 g C m^{-2} d^{-1} at RK 0 and reached a minimum of less than 0.01 g C m^{-2} d^{-1} at RK 102 where it remained for the last 58 km. Unlike the two previous simulations, there was no riparian corridor and therefore this trend of primary production was dictated solely by the trends of channel depth (Figure 3B) and K_d (Figure 4A). Without a forested canopy, there was no effect of channel orientation on GPP, and thus inter-sectional variability was caused solely by topography. Compared to the pre-agricultural simulation, GPP in this simulation had a much higher peak that was shifted 52 km upstream all the way to the headwaters.

The consequences of altered light availability associated with agricultural land-use scenarios were extremely pronounced for primary production at the scale of the entire river. When summed

over the entire channel length, estimated pre-agricultural GPP (4992 kg C d^{-1}) was over seven times higher ($P < 0.01$) than both post-agricultural scenarios and the present-day river configuration (Figure 9). Pre-agricultural, whole-river GPP for a completely overcast day was even higher than present-day, whole-river GPP for a full sun day. As expected, high turbidity with an intact forested riparian zone resulted in the lowest estimate of GPP. However, whole-river GPP was not statistically different among the three post-agricultural scenarios ($P = 0.49$).

DISCUSSION

Basin-Scale Benthic Light Availability

Along the river continuum, channel geometry (Figure 3; Leopold and Maddock 1953) and water clarity (Figure 4; Julian and others 2008a) display a high degree of organization. These longitudinal trends of hydrogeomorphic controls provided the foundation on which our basin-scale BLAM was built. Using this model, we were able to estimate benthic PAR (E_{bed}) along a 160-km free-flowing mainstem channel in an agriculturally dominated basin. Overall, E_{bed} decreased in the downstream direction due primarily to increasing water column turbidity, and there was considerable local variation caused by changes in topography, riparian vegetation, and channel orientation.

The qualitative expectation of light availability proposed in the River Continuum Concept (RCC; Vannote and others 1980) is a parabolic distribution in which light is low in the upper and lower reaches, and high in the middle reaches, reflecting a transition from shading by riparian vegetation giving way to aquatic light attenuation by increasing turbidity in larger river reaches. We found a similar pattern for the pre-agricultural simulation of the Baraboo River with an intact-forested riparian corridor and pristine water clarity. The peak in this curve at RK 52 is the point along the river where the combined effects of terrestrial shading and aquatic attenuation were at a minimum. This point therefore signifies a threshold where terrestrial shading is the dominant control of E_{bed} upstream of the peak and aquatic attenuation is the dominant control of E_{bed} downstream of the peak. Statistical evidence for this relationship of dominant controls on E_{bed} is presented in Julian and others (2008b).

Although the longitudinal profile in E_{bed} for the pristine river scenario was consistent with conventional wisdom, the trend was not smooth, and light availability remained relatively high at the base of the drainage where the sixth-order channel had an estimated depth of 1.6 m (Figure 7B, curve 1). The considerable inter-sectional variability was due primarily to changes in orientation of the highly sinuous channel, and, to a lesser degree, shading by adjacent hills. Thus, in this pre-disturbance scenario, channel and landform geomorphology create local heterogeneities in light availability which can cause similar patchiness in benthic primary production. The significance of these geomorphic controls should certainly vary as a function of regional topography (which dictates both topographic shading and channel form), but the magnitude of these effects is yet to be quantified within and across diverse river systems. In all, the longitudinal trend in E_{bed} as proposed by the RCC is only valid for rivers with a continuously forested riparian corridor, pristine water clarity, and no sinuosity.

The scenario of pristine water conditions and intact riparian forests is increasingly rare in worldwide rivers. Most landscapes have been affected by some degree of anthropogenic disturbance, which often increases turbidity (Walling and Fang 2003; MEA 2005) and is associated with reduced riparian forest extent in regions where such plant communities would normally be present (MEA 2005). Our second and third modeling scenarios were intended to illustrate how two common consequences of agricultural land use—accelerated soil erosion and conversion of riparian forests for farming—alter longitudinal profiles of benthic light availability and GPP.

In scenario 2, which represents the Baraboo River after agricultural land conversion but before removal of any riparian forests, the peak in E_{bed} was reduced and shifted upstream. This reduction and upstream shift in E_{bed} results from increased water column turbidity and consequently the dominance of aquatic light attenuation on E_{bed}. Turbidity values in Baraboo River are by no means the highest for agricultural streams, and thus the longitudinal trend in E_{bed} could potentially have a lower peak that is shifted even farther upstream for streams impacted by enhanced agricultural runoff.

The third scenario represents the Baraboo River after agricultural land conversion and complete removal of riparian forests, and resulted in the parabolic trend in E_{bed} shifting to a logarithmic trend in which E_{bed} was much greater in the headwaters and decreased rapidly along the river continuum. With the absence of riparian shading, aquatic light attenuation became the dominant control on E_{bed} for the entire continuum. In addi-

tion to changing the longitudinal distribution of E_{bed}, this scenario also eliminated all inter-sectional variability caused by channel orientation. For a river with a mixed riparian community such as Baraboo River, the curve in scenario 3 represents the upper limit of E_{bed} whereas the curve in scenario 2 represents the lower limit of E_{bed}. Comparison of the four curves in Figure 7 illustrates that agricultural land use is likely to (i) increase the magnitude of E_{bed} near the headwaters due to riparian deforestation, (ii) decrease the magnitude of E_{bed} in the lower reaches due to increased turbidity, (iii) shift the peak in E_{bed} upstream due to increased dominance of aquatic light attenuation over terrestrial shading, and (iv) increase reach-scale variability in E_{bed} due to a discontinuous riparian community.

Agricultural Landscapes and Primary Production

Given the shape of the P–I curves used, GPP estimates generally mirrored E_{bed} for current and simulated conditions in the Baraboo River. However, three consequences of agricultural land use on GPP are worth emphasizing. First, GPP estimated for the actual configuration of the Baraboo River (Figure 8A) is characterized by substantial variation over very short distances, and this spatial variability is likely to have important consequences for community composition and densities of higher trophic levels (Hawkins and others 1982; Hawkins 1986). Second, in all post-agricultural scenarios, GPP is shifted from having a relatively steady rate (between 1 and 2 g C m^{-2} d^{-1}) throughout the majority of the 160 km system to having a skewed distribution with high productivity in headwater reaches and undetectable rates in the last 60 km (38%) of the river. This represents a substantial redistribution and absence of a critical resource for lotic consumers. The final and most conspicuous consequence of agricultural land use is the remarkable overall reduction in GPP for the entire river (Figure 9). Even in highly heterotrophic ecosystems, benthic algal production is often the dominant energy source supporting higher trophic levels in food webs (Mayer and Likens 1987; McNeely and others 2007). Thus, the disappearance of this energy source due to light limitation should have important consequences for secondary production and community composition, in addition to likely modification of photochemical processes, nutrient uptake, thermal regimes, and other light-affected ecological processes in agriculturally influenced streams and rivers.

Model Constraints and Future Considerations

Several potential limitations need to be acknowledged in our model estimates of light and GPP. First, we used a traditional approach of defining the study system as an uninterrupted, linear channel. The absence of dams or other major engineering alterations allowed us to treat the Baraboo River as a seamless continuum, which is not characteristic of most rivers (Nilsson and others 2005). Most fluvial systems have longitudinal "discontinuities" caused by dams (Smith and others 2002), geomorphic heterogeneity (Montgomery 1999), and confluences (Rhoads 1987; Kiffney and others 2006). An emerging paradigm in fluvial geomorphology and ecology is conceptualizing the river as a series of network links rather than a continuum (Rice and others 2001; Benda and others 2004). Indeed, Julian and others (2008a) found that the water clarity of Baraboo River along its continuum was heavily influenced by tributary inputs. Although basin network configuration does influence aquatic light attenuation along the river, terrestrial shading is only dictated by the local controls of topography and riparian vegetation. Our approach of using DEMs and LCMs to quantify terrestrial shading could be applied to entire river networks, although it would require more extensive empirical data to assess broad spatial variations in y and K_d.

Second, simulating pristine conditions is inherently limited by the absence of information from the Baraboo River prior to human influence, or the ability to use an adjacent undisturbed basin as a reference site because all rivers in the region are affected by agricultural land use. Spatially extensive data on optical water quality in rivers of any sort are extremely scarce, which limited our opportunities for scenario development. We assumed that water clarity for the Motueka River, NZ provided a reasonable representation of what water conditions would have been like in the Baraboo River prior to land-use conversion because of similarities in the size and shape of the two basins. Because factors such as climate and parent geology (which obviously differ between Wisconsin, USA and New Zealand) affect turbidity in pristine rivers, using the Motueka data clearly introduced some unknown amount of error into our estimates of E_{bed} and GPP. However, we suggest that differences in turbidity between the Motueka River and a pre-disturbance Baraboo River are likely to be small in comparison to the difference between water clarity for the pre-disturbance and present-day Baraboo. In this case, the introduced error should not sub-

stantially alter the result of major differences in the light regimes of the pristine and disturbed Baraboo River.

Our examination of light and production in the Baraboo River emphasized spatial variability but not temporal variability. By confining our analyses to summer and baseflow conditions, we minimized temporal variability in riparian shading and aquatic light attenuation, respectively. Although we used baseflow water clarity from one day, these values do not change appreciably during baseflow conditions (Julian and others 2008a) and; therefore, our values of K_d were characteristic of the average summer day during baseflow. To characterize temporal variability in aquatic light attenuation, greater sampling across a wide range of flows would be needed (for example, Julian and others 2008a). Flow variability combined with constantly changing weather produces tremendous temporal variation in metabolism on daily, seasonal, inter-storm, and inter-year scales (Roberts and others 2007), and along with a need to understand how geomorphology constrains light availability, how these temporal dynamics intersect with spatial patterns and controls remains to be explored.

A final assumption built into our study was the prediction of GPP from light profiles alone; that is, that light is the primary constraint on GPP in the Baraboo River. Multiple factors can limit metabolism in streams, and substantial attention has been given to nutrient availability as a control on algal growth in particular (Hilton and others 2006). However, nutrient limitation becomes important only if sufficient light is present (Greenwood and Rosemond 2005; Lin and others 2007; Von Schiller and others 2007). And because nutrient and sediment enrichment are common consequences of agricultural land use (for example, Johnson and others 1997; Robertson and others 2006), we suggest that light availability is likely to be the dominant limitation on benthic production at the basin scale.

CONCLUSIONS

There are several widespread anthropogenic disturbances that alter the light regimes of rivers including urbanization, logging, mining, dam construction and removal, and point source discharges. How these land-use changes affect light availability is not necessarily straightforward, and are likely to be spatially and temporally dynamic. For example, urbanization increases the turbidity of rivers through increased soil runoff (Wolman 1967) and decreases terrestrial shading through riparian deforestation and channel widening associated with channel evolution following increased surface water runoff (Hammer 1972). These geomorphic changes from channel evolution usually extend upstream and downstream of the urban-impacted area (Graf 1975; Simon 1992). However, channel widening is typically preceded by channel incision (Harvey and others 1984). This entrenchment not only increases topographic shading of the channel, but also increases vegetation shading by causing riparian trees to lean toward the center of the channel, which we observed in some of the lower sections of Baraboo River. Thus, urbanization is likely to (i) increase E_{bed} in some reaches due to reduced vegetation shading, (ii) decrease E_{bed} in others due to enhanced aquatic light attenuation or enhanced topographic shading, and (iii) increase the variability of E_{bed} along the river continuum due to spatial and temporal discontinuities of the previous two effects.

Similar scenarios can and should be generated and tested for a range of basin land uses. Understanding how these and other disturbances alter light availability in rivers is a critical step in managing streams and rivers, as it should help identify times and places of degraded water quality and increased algal growth. This argument is based on the results of this study which illustrate profound changes in light availability in response to human land use, and the significance of light limitation on lotic algal growth at the basin scale. Indeed, the importance of light in modulating riverine eutrophication has largely been overlooked by researchers and managers (Von Schiller and others 2007). We expect that application of reach- and basin-scale light availability models such as was done here should provide new insights into light limitation and guide management of eutrophic streams and rivers.

ACKNOWLEDGMENTS

REFERENCES

Alexander RB, Smith RA. 2006. Trends in nutrient enrichment of U.S. rivers during the 20th century and their relation to probable stream trophic conditions. Limnol Oceanogr 51: 639–54.

Basher LR. 2003. The Motueka and Riwaka catchments: a technical report summarising the present state of knowledge of the catchments, management issues and research needs for integrated catchment management. Lincoln: Manaaki Whenua Landcare Research, p 122.

Benda L, Poff NL, Miller D, Dunne T, Reeves G, Pess G, Pollock M. 2004. The network dynamics hypothesis: how channel networks structure riverine habitats. BioScience 54:413–27.

Curtis JT. 1959. The vegetation of Wisconsin. Madison: The University of Wisconsin Press.

Davies-Colley RJ. 1990. Frequency distributions of visual water clarity in 12 New Zealand rivers. NZ J Marine Freshw Res 24:453–60.

Davies-Colley RJ, Vant WN, Smith DG. 2003. Colour and clarity of natural waters. New York: Ellis Horwood.

Dodds WK, Biggs BJF, Lowe RL. 1999. Photosynthesis-irradiance patterns in benthic microalgae: variations as a function of assemblage thickness and community structure. J Phycol 35:42–53.

Dodds WK, Welch EB. 2000. Establishing nutrient criteria in streams. J N Am Benthol Soc 19:186–96.

Frazer GW, Canham CD, Lertzman KP. 1999. Gap light analyzer (GLA), version 2.0: imaging software to extract canopy structure and gap light transmission indices from true-colour fisheye photographs, users manual and program documentation. Burnaby, B.C. and Millbrook, NY: Simon Fraser University and Institute of Ecosystem Studies, p 40.

Fu P, Rich PM. 2000. The Solar Analyst 1.0 manual. HELIOS Environmental Modeling Institute, USA, pp. 53.

Graf WL. 1975. The impact of suburbanization on fluvial geomorphology. Water Resour Res 11:690–2.

Greenwood JL, Rosemond AD. 2005. Periphyton response to long-term nutrient enrichment in a shaded headwater stream. Can J of Fish Aquat Sci 62:2033–45.

Hammer TR. 1972. Stream channel enlargement due to urbanization. Water Res Res 8:1530–40.

Harvey MD, Watson CC, Schumm SA. 1984. Channelized streams: an analog for the effects of urbanization. In: Sterling H.J., Ed. International symposium on urban hydrology, hydraulics and sediment control. Lexington, KY: University of Kentucky. p 401–9.

Hawkins CP. 1986. Variation in individual growth rates and population densities of ephemerellid mayflies. Ecology 67:1384–95.

Hawkins CP, Murphy ML, Anderson NH. 1982. Effects of canopy, substrate composition, and gradient on the structure of macroinvertebrate communities in Cascade Range streams of Oregon. Ecology 63:1840–56.

Hilton J, O'Hare M, Bowes MJ, Jones JI. 2006. How green is my river? A new paradigm of eutrophication in rivers. Sci Total Environ 365:66–83.

Jassby AD, Platt T. 1976. Mathematical formulation of the relationship between photosynthesis and light for phytoplankton. Limnol Oceanogr 21:540–7.

Johnson LB, Richards C, Host GE, Arthur JW. 1997. Landscape influences on water chemistry in Midwestern stream ecosystems. Freshw Biol 37:193–208.

Julian JP, Doyle MW, Powers SM, Stanley EH, Riggsbee JA. 2008a. Optical water quality in rivers. Water Resour Res. doi:10.29/2007WR006457, in press.

Julian JP, Doyle MW, Stanley EH. 2008b. Empirical modeling of light availability in rivers. J Geophys Res Biogeosci 113:G03022. doi:10.1029/2007JG000601.

Kiffney PM, Greene CM, Hall JE, Davies JR. 2006. Tributary streams create spatial discontinuities in habitat, biological productivity, and diversity in mainstem rivers. Can J Fish Aquat Sci 63:2518–30.

Leopold LB, Maddock T Jr. 1953. The hydraulic geometry of stream channels and some physiographic implications. USGS Professional Paper 252, pp 1–57.

Lin LS, Markus M, Russell A. 2007. Stream classification system based on susceptibility to algal growth response to nutrients. J Environ Eng 133:692–7.

Maidment DR. 2002. Arc hydro: GIS for water resources. Austin: Center for Research in Water Resources, University of Texas.

Mayer MS, Likens GE. 1987. The importance of algae in a shaded headwater stream as food for an abundant caddisfly (Trichoptera). J N Am Benthol Soc 6:262–9.

McNeely C, Finlay JC, Power ME. 2007. Grazer traits, competition, and carbon sources to a headwater stream food web. Ecology 88:391–401.

Millennium Ecosystem Assessment (MEA). 2005. Ecosystems and human well-being: synthesis. Washington, DC: Island Press.

Montgomery DR. 1999. Process domains and the river continuum. J Am Water Resour Assoc 35:397–410.

Nilsson C, Reidy CA, Dynesius M, Revengz C. 2005. Fragmentation and flow regulation of the world's large river systems. Science 308:405–8.

Osterkamp WR, Hedman ER. 1977. Variation of width and discharge for natural high-gradient stream channels. Water Resour Res 13:256–8.

Rhoads BL. 1987. Changes in stream channel characteristics at tributary junctions. Phys Geogr 8:346–61.

Rice SP, Greenwood MT, Joyce CB. 2001. Tributaries, sediment sources, and the longitudinal organisation of macroinvertebrate fauna along river systems. Can J Fish Aquat Sci 58:824–40.

Roberts BJ, Mulholland PJ, Hill WR. 2007. Multiple scales of temporal variability in ecosystem metabolism rates: results from 2 years of continuous monitoring in a forested headwater stream. Ecosystems 10:588–606.

Robertson DM, Graczyk DJ, Garrison PJ, Wang L, LaLiberte G, Bannerman R. 2006. Nutrient concentrations and their relations to the biotic integrity of wadeable streams in Wisconsin. U.S. Geological Survey Professional Paper 1722.

Scudder BC, Stewart JS. 2001. Benthic algae of benchmark streams in agricultural areas of Eastern Wisconsin. Middleton, WI: U.S. Geological Survey, p 54.

Simon A. 1992. Energy, time, and channel evolution in catastrophically disturbed fluvial systems. Geomorphology 5:345–72.

Smith SV, Renwick WH, Bartley JD, Buddemeier RW. 2002. Distribution and significance of small, artificial water bodies across the United States. Sci Total Environ 299:21–36.

U.S. Department of Agriculture (USDA). 2007. UV-B Monitoring and Research Program, http://uvb.nrel.colostate.edu/UVB/.

Vannote RL, Minshall GW, Cummins KW, Sedell JR, Cushing CE. 1980. The river continuum concept. Can J Fish Aquat Sci 37:130–7.

Von Schiller D, Marti E, Riera JL, Sabater F. 2007. Effects of nutrients and light on periphyton biomass and nitrogen uptake in Mediterranean streams with contrasting land use. Freshw Biol 52:891–906.

Walling DE, Fang D. 2003. Recent trends in the suspended sediment loads of the world's rivers. Global Planet Change 39:111–26.

Wisconsin Department of Natural Resources (WDNR). 2006. Wisconsin Dam Database, http://dnr.wi.gov/org/water/wm/dsfm/dams/datacentral.html.

Wisconsin Department of Natural Resources (WDNR). 1998. Landcover Data (WISCLAND), http://dnr.wi.gov/maps/gis/datalandcover.html.

Wolman MG. 1967. A cycle of sedimentation and erosion in urban river channels. Geografiska Annaler 49A:385–95.